

## MOLAR HEAT CAPACITY AND THERMODYNAMIC PROPERTIES OF 1,2-CYCLOHEXANE DICARBOXYLIC ANHYDRIDE [C<sub>8</sub>H<sub>10</sub>O<sub>3</sub>]

X.-C. Lv<sup>1</sup>, X.-H. Gao<sup>1</sup>, Z.-C. Tan<sup>2,3\*</sup>, Y.-S. Li<sup>3</sup> and L.-X. Sun<sup>2</sup>

<sup>1</sup>School of Chemistry and Material Science, Liaoning Shihua University, Fushun 113001, China

<sup>2</sup>Thermochemistry Laboratory, Dalian Institute of Chemical Physics, Chinese Academy of Science, Dalian 116023, China

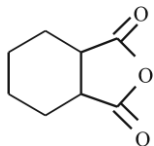
<sup>3</sup>College of Environmental Science & Engineering, Dalian Jiaotong University, Dalian, 116028, China

The molar heat capacity  $C_{p,m}$  of 1,2-cyclohexane dicarboxylic anhydride was measured in the temperature range from  $T=80$  to 390 K with a small sample automated adiabatic calorimeter. The melting point  $T_m$ , the molar enthalpy  $\Delta_{fus}H_m$  and the entropy  $\Delta_{fus}S_m$  of fusion for the compound were determined to be 303.80 K, 14.71 kJ mol<sup>-1</sup> and 48.43 J K<sup>-1</sup> mol<sup>-1</sup>, respectively. The thermodynamic functions [ $H_T - H_{273.15}$ ] and [ $S_T - S_{273.15}$ ] were derived in the temperature range from  $T=80$  to 385 K with temperature interval of 5 K. The thermal stability of the compound was investigated by differential scanning calorimeter (DSC) and thermogravimetry (TG), when the process of the mass-loss was due to the evaporation, instead of its thermal decomposition.

**Keywords:** adiabatic calorimetry, 1,2-cyclohexane dicarboxylic anhydride, low-temperature heat capacity, thermal analysis

### Introduction

1,2-Cyclohexane dicarboxylic anhydride (CAS No.: 85-42-7), is also named hexahydrophthalic anhydride (abbreviated to HHPA). Its molecular formula is C<sub>8</sub>H<sub>10</sub>O<sub>3</sub>, the molar mass is 154.17 g mol<sup>-1</sup> and the structural formula is



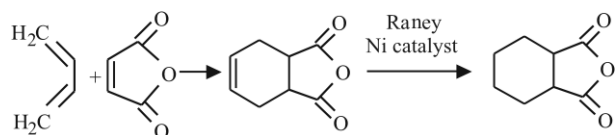
The HHPA is curing agent for epoxy resin. Curing agents for epoxy resins promote attractive characteristics of high tensile strength and modulus, low shrinkage on curing, high resistance to chemicals and corrosion, excellent dimensional stability, and superior electrical properties [1, 2]. Although epoxy resin can be cured with different hardeners, most studies performed to date have been devoted to different aspects related to epoxy resins cured with amine curing agents, and few of papers have been devoted to epoxy/anhydride mixtures. In fact, anhydride-like curing agents are preferred for electrical and electronic applications or when chemical safety has to be taken into account [3]. Besides being used as a curing agent for epoxy resin, HHPA is also used as an intermediate in the preparation of many pesticides and herbicides. However, the thermodynamic data of HHPA have not been reported up to now.

Because this kind of compounds is very useful in many fields, for the purpose of their application, in previous works, we had studied the 3,4,5,6-THPA and 4-MTHPA, in the present paper a thermodynamic study was performed including heat capacity and thermal stability of HHPA.

### Experimental

#### Sample

The sample used in these experiments was provided by Huicheng Chemicals Co. of China and synthesized by the following procedures. Briefly, C (THPA) is synthesized with A (butadiene) and B (maleic acid anhydride) in terms of Diels Alder Reaction and D (HHPA) is obtained by the hydrogenation of C (THPA).



#### Adiabatic calorimetry

A precision automatic adiabatic calorimeter was used to measure the heat capacities of the compound over the temperature range between  $T=78$  and 390 K. The instrument was established in Thermochemistry Laboratory of Dalian Institute of Chemical Physics, Chinese Academy of Sciences.

\* Author for correspondence: tzc@dicp.ac.cn

The structure and principle of the adiabatic calorimeter have been described in detail elsewhere [4–6]. The automatic adiabatic calorimeter mainly consisted of a sample cell made of gold-plated copper, a miniature platinum resistance thermometer (IPRT No. 2, produced by Shanghai Institute on Industrial Automatic Meters, 16 mm in length, 1.6 mm in diameter and a nominal resistance of  $100\ \Omega$ ), an electric heater, the inner and the outer adiabatic shields, two sets of six-junctions chromel-constantan thermopiles installed between the calorimetric cell and the inner shield and between the inner and the outer shields, respectively, and a high vacuum can [7–9].

The effective capacity of the sample cell was  $6\text{ cm}^3$ . Four gold-plated copper canes of 0.2 mm in thickness placed inside with an X-shape to promote heat distribution. A miniature platinum thermometer was inserted into a horizontal copper sheath soldered under the bottom. The thermometer was calibrated on the basis of ITS-90 by the Station of Low-temperature Metrology and Measurements, Academia Sinica. The resistance of the thermometer was measured by a 71/2 Digit Nano Volt/Micro Ohm meter (Model 34420, Agilent, USA). The heater wire was bifilarly wound and fixed around outside the wall of the sample cell. After the sample was loaded, the cell was sealed and evacuated. A small amount of helium gas ( $0.1\text{ MPa}$ ) was introduced into the cell so as to enhance the heat transfer.

The temperature difference between sample cell and inner shield, and between inner and outer shield were monitored by two sets of thermocouples. Both shields were heated under the control of Temperature Controller (Model 340, Lakeshore, USA) and kept at the same temperatures as that of the sample cell. The electrical energy introduced into the sample cell was automatically picked up by a Data Acquisition/Switch Unit (Model 34970A, Agilent, USA). The equilibrium temperature of the cell after the energy input was measured by the 71/2 digit Nano Volt/Micro ohm meter. The energy and the temperature data were processed on line by a computer.

The heat capacity measurements were conducted by the standard procedure of intermittently heating the sample and alternately measuring the temperature. The heating rate was  $0.1$  to  $0.4\text{ K min}^{-1}$ ; the temperature increments of the experimental points were between 1 and 4 K; the heating duration was 10 min and the temperature drift rates of the sample cell, which was measured in an equilibrium period, were kept within  $10^{-3}$  to  $10^{-4}\text{ K min}^{-1}$ .

Prior to the heat capacity measurement of the sample, the molar heat capacities of  $\alpha\text{-Al}_2\text{O}_3$ , the standard reference material, were measured from  $T=78$  to  $400\text{ K}$  to verify the reliability of the adiabatic calorimeter. The

results showed that the deviation of our calibration data from those of NIST [10] was within  $\pm 0.3\%$ .

In the present paper, the mass of HHPA used for the measurement was  $2.5008\text{ g}$ , which was equivalent to  $0.0162\text{ mol}$  based on the molar mass  $M=154.17\text{ g mol}^{-1}$ .

### Thermal analysis

A differential scanning calorimeter (DSC-141, Setaram, France) was used to perform the thermal analysis of HHPA at the heating rate of  $10\text{ K min}^{-1}$  under a purity nitrogen with flowing rate of  $50\text{ mL min}^{-1}$ . The mass of the sample used in the experiment was  $4.2\text{ mg}$ . The calibrations for the temperature and heat flux of the calorimeter were performed prior to the experiment. The temperature scale was calibrated by measuring the melting points of Hg, In, Sn, Pb and Zn, at different heating rates, and the heat flux was calibrated by the Joule effect. Measurement of the melting temperature and the enthalpy of fusion of benzoic acid (NIST, Standard Reference Material 39i) were made in our laboratory to check the accuracy of the instrument.

The TG measurement of the sample was carried out by a thermogravimetric analyzer (Model: DT-20B, Shimadzu, Japan) at the heating rate of  $10\text{ K min}^{-1}$  under a purity nitrogen with flow rate of  $30\text{ mL min}^{-1}$ . The mass of the sample used in the experiment was  $7.2\text{ mg}$ . The reference crucible was filled with  $\alpha\text{-Al}_2\text{O}_3$ . The TG-DTG equipment was calibrated by the SRM in the thermal analysis,  $\text{CaC}_2\text{O}_4\cdot\text{H}_2\text{O(s)}$ .

## Results and discussion

### *Molar heat capacity and thermodynamic functions*

The experimental molar heat capacities,  $C_{\text{p,m}}$  of HHPA were shown in Fig. 1 and listed in Table 1 from  $T=80$  to  $390\text{ K}$ .

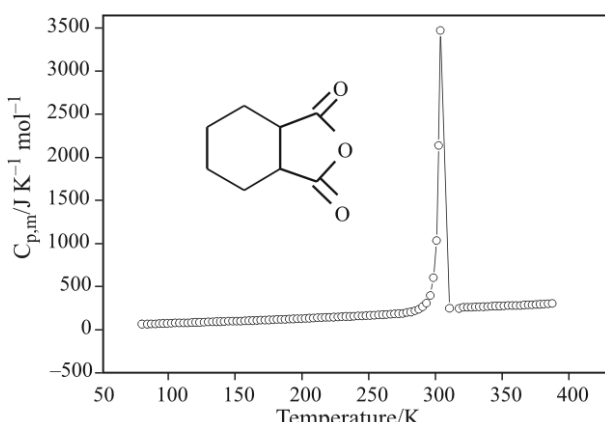


**Fig. 1** Experimental molar heat-capacity plotted vs. temperature for HHPA

**Table 1** Experimental molar heat capacities, ( $C_{p,m}$ ), of HHPA( $C_8H_{10}O_3$ )

$T/K$	$C_{p,m}/J\text{ K}^{-1}\text{ mol}^{-1}$	$T/K$	$C_{p,m}/J\text{ K}^{-1}\text{ mol}^{-1}$
80.341	63.265	160.278	103.82
84.343	64.738	163.231	105.53
87.245	66.393	166.201	107.32
90.247	67.914	169.221	109.00
93.162	69.659	172.338	110.80
96.169	71.084	175.455	112.66
99.267	72.567	178.523	114.57
102.293	73.871	181.542	116.76
105.252	75.691	184.562	118.48
108.306	77.040	187.532	120.46
111.452	78.615	190.503	122.29
114.537	80.552	193.438	124.16
117.567	81.788	196.445	126.21
120.543	83.372	199.562	128.44
123.613	85.112	202.630	130.64
126.774	86.676	205.649	133.16
129.884	88.254	208.669	135.07
132.951	89.497	211.688	137.26
135.974	91.238	214.659	139.17
138.958	92.841	217.630	141.29
141.904	94.395	220.649	143.01
144.943	95.919	223.766	145.53
148.075	97.543	226.883	147.25
151.175	99.247	229.903	149.47
154.243	100.66	232.922	151.24
157.275	102.18	235.990	153.33
239.010	155.33	317.767	246.06
241.981	157.65	320.758	258.37
245.049	160.14	323.860	259.63
248.076	162.35	326.867	261.60
251.103	165.02	329.872	262.67
254.202	167.04	332.862	264.08
257.273	169.73	335.843	266.64
260.320	172.55	338.896	268.57
263.340	176.14	342.012	270.24
266.342	179.52	345.118	272.44
269.316	183.34	348.214	273.80
272.368	185.82	351.294	275.62
275.497	187.33	354.361	277.82
278.574	197.71	357.414	279.54
281.590	206.39	360.449	281.37
284.547	218.24	363.466	281.80
287.509	236.20	366.455	285.53
290.437	264.62	369.437	288.22

**Table 1** Continued

$T/K$	$C_{p,m}/J\text{ K}^{-1}\text{ mol}^{-1}$	$T/K$	$C_{p,m}/J\text{ K}^{-1}\text{ mol}^{-1}$
293.271	309.22	372.396	289.31
296.036	397.38	375.336	291.17
298.564	599.63	378.258	294.48
300.761	1033.3	381.235	297.12
302.435	2138.3	384.264	299.95
303.802	3473.0	387.264	303.57
310.512	249.12		

Two polynomial equations were obtained by the least square fitting by using the experimental molar heat capacities ( $C_{p,m}$ ) and the experimental temperatures ( $T$ ).

From  $T=80$  to 274 K (solid phase):

$$C_{p,m} (\text{J K}^{-1} \text{ mol}^{-1}) = 113.77 + 60.352x + 17.479x^2 - 8.6658x^3 - 23.8x^4 + 11.232x^5 + 18.595x^6 \quad (1)$$

where  $x = [(T/\text{K}) - 177]/97$ ,  $x$  is the reduced temperature, 177 is obtained from polynomial  $(T_{\max} + T_{\min})/2$ , 97 is obtained from polynomial  $(T_{\max} - T_{\min})/2$ ,  $T_{\max}$  is the upper limit of the above temperature region,  $T_{\min}$  is the lower limit of the above temperature region, and  $T$  is the experimental temperature. Correlation coefficient  $R^2$  of least square fitting is 0.9999. The relative deviations of the smoothed heat capacities from those obtained from the experiment were within  $\pm 0.3\%$ .

From  $T=318$  to 388 K (liquid phase):

$$C_{p,m} (\text{J K}^{-1} \text{ mol}^{-1}) = 276.79 + 21.099x + 0.3853x^2 + 2.6008x^3 + 3.6278x^4 \quad (2)$$

where  $x = [(T/\text{K}) - 353]/35$ , its correlation coefficient  $R^2$  is 0.9989.

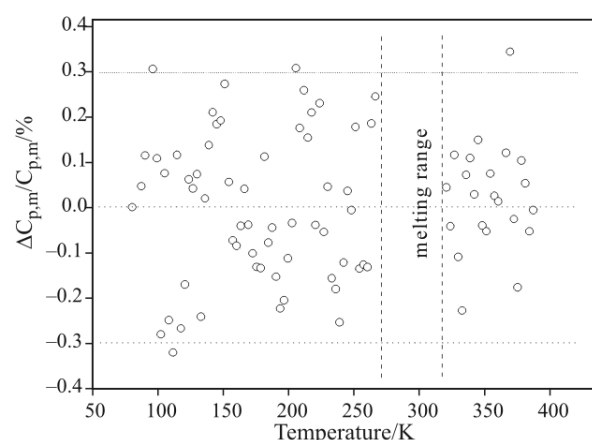


**Fig. 2** The plot of relative deviations of the experimental heat capacity values of the sample,  $C_{p,m}(\text{expt})$ , from the fitting heat-capacity values,  $C_{p,m}(\text{fit})$ , vs. the absolute temperature ( $T$ ). [ $\Delta C_{p,m} = C_{p,m}(\text{expt}) - C_{p,m}(\text{fit})$ ]

The relative deviations of the smoothed heat capacities from those obtained from the experiment were shown in Fig. 2. It gives the plot of relative deviations of the experimental heat capacity values of the sample,  $C_{p,m}(\text{expt})$ , from the fitting heat-capacity values,  $C_{p,m}(\text{fit})$ , *vs.* the absolute temperature ( $T$ ). It can be seen from Fig. 2 that relative deviations of all the experimental points from the fitting heat-capacity values are within  $\pm 0.3\%$  in the solid phase region.

From Fig. 1, it can be seen that HHPA melted from  $T=274$  to 318 K with the peak temperature  $T=303.80$  K. The molar enthalpy  $\Delta_{\text{fus}}H_m$  and entropy  $\Delta_{\text{fus}}S_m$  of fusion of the compound were derived according to the following Eqs (3) and (4) :

$$\Delta H_m = \left[ Q - n \int_{T_i}^{T_m} C_p(s) dT - n \int_{T_m}^{T_f} C_p(L) dT - \int_{T_i}^{T_f} H_0 dT \right] / n \quad (3)$$

$$\Delta S_m = \Delta H_m / T_m \quad (4)$$

where  $T_i$  is the temperature a few degrees lower than the initial melting temperature,  $Q$  the total energy introduced into the sample cell from  $T_i$  to  $T_f$ ,  $T_f$  a temperature slightly higher than the final melting temperature,  $C_p(s)$  the heat capacity of the sample in the solid phase from  $T_i$  to  $T_m$ ,  $C_p(L)$  the heat capacity of the sample in liquid phase from  $T_m$  to  $T_f$ .

The values of melting temperature  $T_m$ , molar enthalpy,  $\Delta_{\text{fus}}H_m$ , and entropy of fusion,  $\Delta_{\text{fus}}S_m$ , of the sample were determined to be 303.80 K, 14.71 kJ mol<sup>-1</sup> and 48.43 J K<sup>-1</sup> mol<sup>-1</sup> from these equations.

In terms of the polynomials of heat capacity and the thermodynamic relationship, the thermodynamic

**Table 2** Continued

$T/K$	$C_{p,m}/$ $J \text{ mol}^{-1} \text{ K}^{-1}$	$(H_T - H_{273.15})/$ $\text{kJ mol}^{-1}$	$(S_T - S_{273.15})/$ $\text{J mol}^{-1} \text{ K}^{-1}$
150	98.359	-16.988	-80.148
155	101.01	-16.489	-76.877
160	103.75	-15.978	-73.623
165	106.58	-15.452	-70.385
170	109.51	-14.912	-67.159
175	112.53	-14.357	-63.941
180	115.65	-13.786	-60.728
185	118.86	-13.200	-57.518
190	122.14	-12.597	-54.307
195	125.49	-11.978	-51.094
200	128.88	-11.343	-47.878
205	132.31	-10.690	-44.656
210	135.75	-10.020	-41.428
215	139.18	-9.3324	-38.194
220	142.62	-8.6280	-34.955
225	146.04	-7.9065	-31.711
230	149.47	-7.1680	-28.462
235	152.92	-6.4123	-25.209
240	156.43	-5.6393	-21.952
245	160.04	-4.8486	-18.690
250	163.85	-4.0393	-15.421
255	167.95	-3.2105	-12.140
260	172.47	-2.3601	-8.8425
265	177.59	-1.4859	-5.5173
270	183.50	-0.5842	-2.1506
273.15	187.74	0.0000	0.0000
275–315	Melting range	Melting range	Melting range
320	257.93	14.517	47.793
325	260.31	15.812	51.961
330	263.03	17.120	56.055
335	265.94	18.443	56.055
340	268.94	19.780	60.099
345	271.97	21.132	64.106
350	274.98	22.499	68.082
355	278.00	23.882	72.031
360	281.05	25.279	75.954
365	284.22	26.692	79.853
370	287.63	28.122	83.733
375	291.42	29.569	87.604
380	295.77	31.037	91.484
385	300.93	32.528	95.403

**Table 2** Thermodynamic functions,  $(H_T - H_{273.15})$  and  $(S_T - S_{273.15})$ , of HHPA ( $\text{C}_8\text{H}_{10}\text{O}_3$ )

$T/K$	$C_{p,m}/$ $J \text{ mol}^{-1} \text{ K}^{-1}$	$(H_T - H_{273.15})/$ $\text{kJ mol}^{-1}$	$(S_T - S_{273.15})/$ $\text{J mol}^{-1} \text{ K}^{-1}$
80	63.126	-22.623	-129.60
85	65.302	-22.303	-125.72
90	67.712	-21.971	-121.92
95	70.260	-21.627	-118.19
100	72.873	-21.270	-114.52
105	75.501	-20.899	-110.90
110	78.115	-20.516	-107.34
115	80.696	-20.119	-103.81
120	83.240	-19.709	-100.33
125	85.753	-19.287	-96.889
130	88.246	-18.852	-93.481
135	90.734	-18.405	-90.105
140	93.236	-17.945	-86.759
145	95.772	-17.473	-83.441

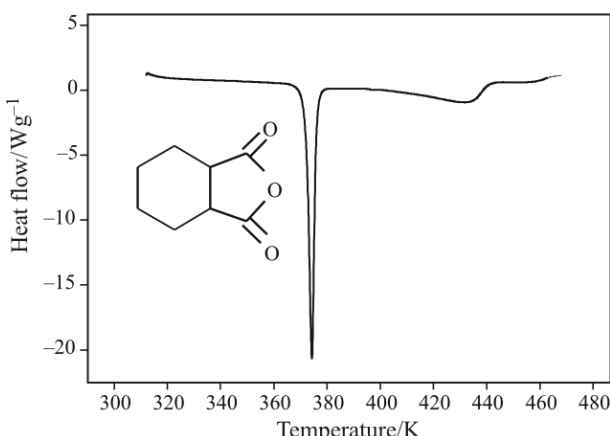


**Fig. 3** DSC curve of HHPA

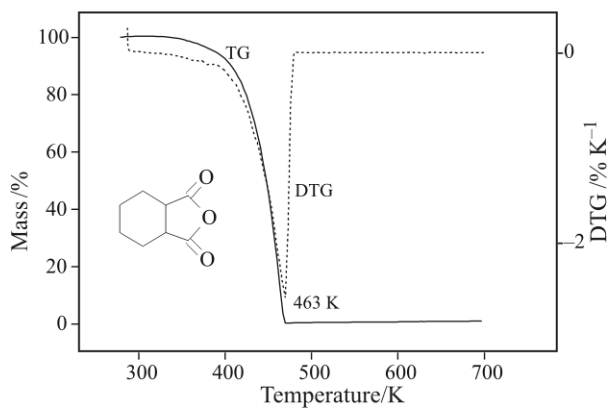


**Fig. 4** TG-DTG curves of HHPA

functions [ $H_T - H_{273.15}$ ] and [ $S_T - S_{273.15}$ ] of the compound were calculated in the temperature range from  $T=80$  to  $385$  K with a temperature interval of  $5$  K and listed in Table 2.

#### *The results of DSC and TG analysis*

The DSC and TG curves of the sample were shown in Figs 3 and 4, respectively.

Based on the DSC curve, the melting temperature, the enthalpy of fusion and entropy of fusion of HHPA were determined to be  $T_m=303.21$  K,  $\Delta_{\text{fus}}H_m=14.59$  kJ mol<sup>-1</sup> and  $\Delta_{\text{fus}}S_m=48.13$  J K<sup>-1</sup> mol<sup>-1</sup>, respectively, which were consistent with that ob-

tained by adiabatic calorimetry,  $303.80$  K,  $\Delta_{\text{fus}}H_m=14.71$  kJ mol<sup>-1</sup> and  $\Delta_{\text{fus}}S_m=48.43$  J K<sup>-1</sup> mol<sup>-1</sup>.

The TG-DTG curves indicated that mass loss of HHPA began at about  $T=383$  K and ended at about  $T=469$  K. It can be seen from Fig. 4 that the maximum mass loss rate of the compound occurred at  $T=463$  K, and the ratio of mass loss was close to 100% after 469 K. Judging from the results of both DSC and TG-DTG, the process of the mass loss of the sample was due to the evaporation, instead of its thermal decomposition.

#### Acknowledgements

This work was financially supported by the National Nature Science Foundation of China under the grant NSFC No. 20373072.

#### References

- 1 G. Lubin, *Handbook of Composites*, Van Nostrand Reinhold, New York 1982, pp. 57–88.
- 2 D. J. Liaw, *J. Polym. Sci., Part A: Polym. Chem.*, 35 (1997) 895.
- 3 P. Guerrero, K. De la Caba, Avalea, M. A. Corcuera and I. Mondragon, *Polymer*, 37 (1996) 2195.
- 4 Z. C. Tan, G. Y. Sun, Y. Sun, *J. Thermal Anal.*, 45 (1995) 59.
- 5 Y. J. Song, Z. C. Tan, S. W. Lu and Y. Xue, *J. Therm. Anal. Cal.*, 77 (2004) 873.
- 6 Z. D. Nan and Z. C. Tan, *J. Therm. Anal. Cal.*, 76 (2004) 955.
- 7 S. X. Wang, Z. C. Tan, Y. Y. Di and F. Xu, *J. Therm. Anal. Cal.*, 76 (2004) 335.
- 8 F. Xu, L. X. Sun, Z. C. Tan, J. G. Liang, Y. Y. Di, Q. F. Tian and T. Zhang, *J. Therm. Anal. Cal.*, 76 (2004) 481.
- 9 B. Xue, J. Y. Wang, Z. C. Tan, S. W. Lu and S. H. Meng, *J. Therm. Anal. Cal.*, 76 (2004) 965.
- 10 D. G. Archer, *J. Phys. Chem. Ref. Data*, 22 (1993) 1441.

Received: June 4, 2007

Accepted: January 11, 2008

DOI: 10.1007/s10973-007-8445-5